Reactions of Malononitrile Dimer with Isothiocyanates

V. V. Dotsenko[a,b,]*, A. V. Bespalov[a], A. A. Russkikh[a], V. K. Kindop[a], N. A. Aksenov[b],
I. V. Aksenova[b], S. V. Shcherbakov[b], and S. N . Ovcharov[b]

[a] Kuban State University, Krasnodar, 350040 Russia
[b] North Caucasus Federal University, Stavropol, 355009 Russia
*e-mail: victor_dotsenko_@mail.ru

Abstract—The reaction of 2-amino-1,1,3-tricyanopropene (malononitrile dimer) with isothiocyanates leads to 1-substituted 4,6-diamino-2-thioxo-1,2-dihydropyridine-3,5-dicarbonitriles or 4,6-diamino-2-(phenylimino)-2*H*-thiopyran-3,5-dicarbonitrile, depending on the conditions. Quantum-chemical modeling of the IR spectra and reaction routes for the synthesized compounds was carried out. *In silico* predictive analysis of potential protein targets, compliance with bioavailability criteria, and ADMET parameters was performed.

Keywords: 2-amino-1,1,3-tricyanopropene, isothiocyanates, heterocyclization, 2*H*-thiopyrans, 2-thioxopyridines, quantum chemical calculations

2-Amino-1,1,3-tricyanopropene **1**, which is readily prepared by the dimerization of malononitrile [1], is a polyfunctional reagent widely used in synthetic organic chemistry. Heterocyclizations involving malononitrile dimer **1** are known since the middle of XX century and are fairly well studied (for reviews, see [2–4]). Nevertheless, there are contradictory data in the literature concerning the regioselectivity of the reactions of malononitrile dimer **1** with isothiocyanates. Thus, Eldin [5] described the reaction of dimer **1** with phenyl isothiocyanate in the presence of a base in DMF, leading to substituted pyridine **2**. The structure of the latter is also confirmed by its S-alkylation, for example, to thienopyridines **3** [6–8] (Scheme 1). At the same time, a similar reaction of dimer **1** with PhNCS in pyridine under reflux leads, according to [9], to substituted pyrimidine **4**. At the same time, it should be noted that the spectral data in [5, 9] do not allow one to unambiguously assign structures **2** or **4** to the products of these reactions.

Continuing research on the chemistry of malononitrile dimer [10–12], we decided to study in detail the regioselectivity of the heterocyclization of 2-amino-1,1,3-tricyanopropene **1** with isothiocyanates and establish the real structure of the resulting compounds. Possible products **2** hold promise as starting reagents for the

synthesis of thieno[2,3-*b*]pyridine derivatives, many of which have pharmacologically useful properties [13–16]. On the other hand, compounds **2–4** are convenient and accessible substrates for preparing S, N-polyheterocyclic assemblies by the Mannich reaction (see, for example, [17–21]).

We reproduced the procedure in [5] to obtain, in a yield of 74%, a product that actually has (according to the IR and NMR spectra) the structure of 4,6-diamino-2-thioxo-1-phenyl-1,2-dihydropyridine-3,5-dicarbonitrile **2** (Table 1, entry 1; Scheme 2). Further studies showed that the reaction of PhNCS with dimer **1**, in principle, does not require harsh conditions similar to those in [5]. For example, pyridine **2** was obtained in 84–92% yields by the reaction of dimer **1** with phenyl isothiocyanate at room temperature in EtOH in the presence of Et₃N (Table 1, entry 2). A similar reaction with allyl isothiocyanate gives 1-allyl-4,6-diamino-2-thioxo-1,2-dihydropyridine-3,5-dicarbonitrile **5** in 58–73% yields (Table 1, entry 6; Scheme 2). The use of stronger bases did not show obvious advantages. For example, the reaction of dimer **1** with allyl isothiocyanate in a superbasic medium (KOH in DMSO), too, leads to the isolation of compound **5** in a yield of 71% (Table 1, entry 7), but the resulting product requires additional purification. Compound **2** is a

Scheme 1.
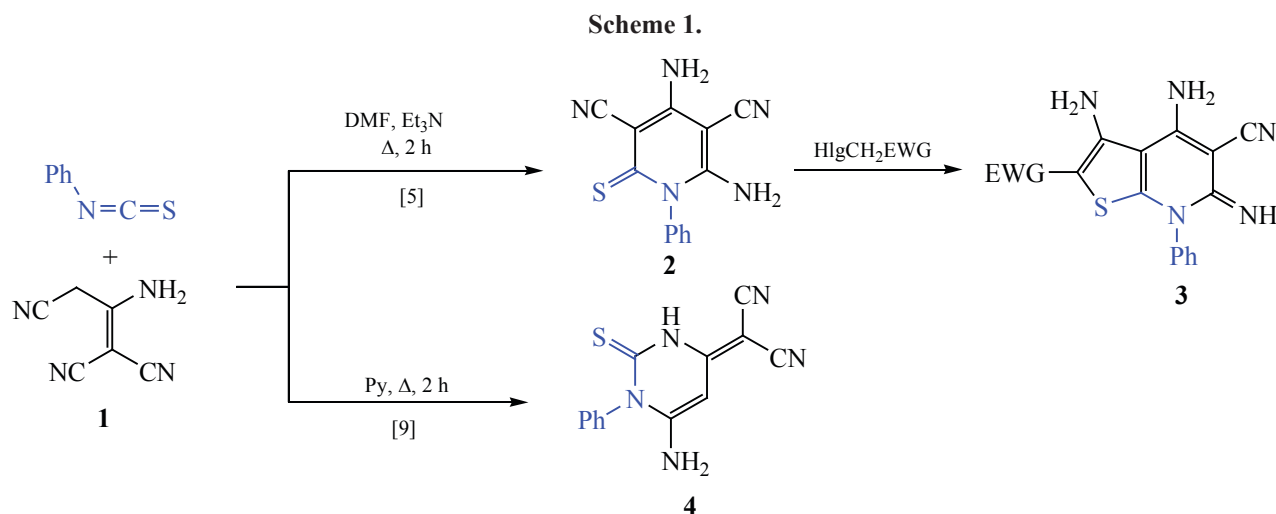
yellow powder insoluble in water and EtOH, moderately soluble in acetone or in an AcOH–DMF mixture under heating. Compound **5** forms colorless crystals soluble in acetone and hot EtOH. The results of all experiments are summarized in Table 1.

Reproducing the method of synthesis of pyrimidine **4**, described by Abdel-Latif et al. [9], gave ambiguous results. One way or another, we failed to obtain both compound **4** and, in general, a product having physicochemical or spectral characteristics reported in [9]. It was found that the direction of the reaction is strongly dependent on its conditions. For example, after the mixture of reagents in pyridine was first allowed to stand at room temperature and then refluxed, we obtained, in a low yield (8%), a beige substance melting above 300 °C and insoluble in boiling EtOH.

Detailed analysis of the spectral data showed that the product is not pyrimidine **4**, and allowed it to be assigned the structure 4,6-diamino-2-(phenylimino)-

2*H*-thiopyran-3,5-dicarbonitrile **6** (Scheme 2; Table 1, entry 3). At the same time, the reaction of malononitrile dimer **1** with PhNCS, when carried out in boiling pyridine from the very beginning, gives a yellow orange product (decomp. point > 300 ° C after purification, instead of the green crystals with mp 225°C, reported in [9]), which, according to the IR and NMR data, is impure 4,6-diamino-2-thioxo-1-phenyl-1,2-dihydropyridine-3,5-dicarbonitrile **2** (Table 1, entry 4).

The reaction of dimer **1** with allyl isothiocyanate in boiling pyridine formed an orange product (yield 37–47%, based on the expected 1 : 1 adduct). The IR spectra of the product showed absorption bands corresponding to stretching vibrations of the N–H group (3323 and 3207 cm^{-1}) and conjugated cyano group (2197 cm^{-1}). However, the synthesized compound could not be characterized by ^{1}H and ^{13}C NMR spectroscopy because of its low solubility in organic solvents, including DMSO.

Table 1. Conditions, yields and products of the reaction of malononitrile dimer **1** with isothiocyanates

Entries	Reagents	Conditions	Reaction product (yield, %)
1	**1**, PhNCS	DMF, Et$_3$N (cat.), reflux 2 h [5]	**2** (74%)
2	**1**, PhNCS	EtOH, Et$_3$N (1–1.5 equiv), 25°C	**2** (84–92%)
3	**1**, PhNCS	Pyridine, 24 h 25°C → reflux, 2 h	**6** (8%)
4	**1**, PhNCS	Pyridine, reflux, 2 h [9]	**2** (48%)
5	**1**, H$_2$C=CHCH$_2$NCS	EtOH, Et$_3$N (cat.), 25°C	No reaction
6	**1**, H$_2$C=CHCH$_2$NCS	EtOH, Et$_3$N (1–1.5 equiv), 25°C	**5** (58–73%)
7	**1**, H$_2$C=CHCH$_2$NCS	DMSO, KOH (1 equiv), 25°C	**5** (71%)
8	**8**, H$_2$C=CHCH$_2$NCS	EtOH, 25°C	**5** (27%)
9	**8**, PhNCS	EtOH, 25°C	**6** (82%)

Scheme 2.


R = Ph (**2**, **6**), allyl (**5**).
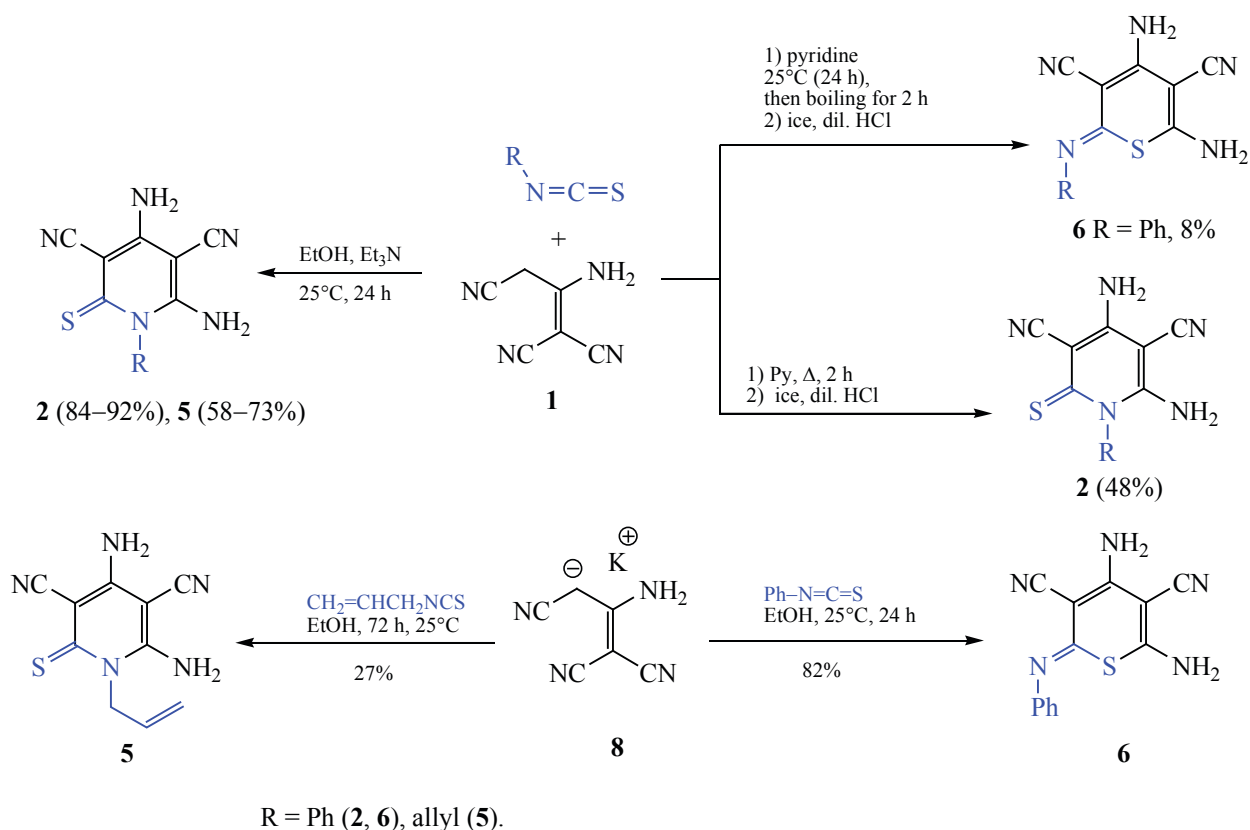
Malononitrile dimer potassium salt **8** reacts with isothiocyanates differently from malononitrile dimer **1**. For example, the reaction of salt **8** with allyl isothiocyanate give the same 1-allyl-4,6-diamino-2-thioxo-1,2-dihydropyridine-3,5-dicarbonitrile **5** but in an appreciably lower yield (27%) (Scheme 2; Table 1, entry 8). At the same time, the reaction of salt **8** with PhN=C=S under analogous conditions leads to thiopyran **6** in a yield of 82% (Table 1, entry 9). It should be noted that we failed to recyclize thiopyran **6** into 2-thioxopyridine **2** even upon prolonged boiling in alcoholic KOH.

Thiopyran **6** has never been described in the literature, but the formation of structurally similar 2H-thiopyrans was previously observed in the reactions of cyclohexylidenemalononitrile with PhNCS [22], ammonolysis of thiopyran salts [23], condensation of malononitrile with enamines β-ketothioanilides [24], and reactions of malononitrile or its dimer with carbon disulfide in the presence of alkalis [25] (Scheme 3).

The structures of 2-thioxopyridines **2** and **5** and 2-iminothiopyran **6** were studied in detail by IR and NMR spectroscopy (¹H, ¹³C DEPTQ, ¹H–¹³C HSQC, ¹H–¹³C

HMBC). The spectra are presented in Supplementary Information.

The ¹H NMR spectra of compounds **2**, **5**, and **6** show signals of the substituent R and broadened signals of two amino groups. The ¹³C (DEPTQ) NMR spectra of all the compounds show signals of two C≡N carbons and 5 characteristic signals of the heteroring carbons. Evidence for the structures is provided by the results of heteronuclear correlation experiments. Thus, the ¹H–¹³C HMBC spectra of compounds **2**, **5**, and **6** contain cross peaks between the protons of one of the amino groups and two signals of the heteroring carbons in the high-field region (C³ and C⁵), which unambiguously confirms the presence of the N≡C–C³=C⁴(NH₂)–C⁵–C≡N fragment (see Supplementary Information). At the same time, the spectra of isomeric compounds **2** and **6** differ from each other in the low-field region: in the spectrum of compound **2**, the pyridine C⁴ and C⁶ signals are observed at 155.6 and 155.9 ppm and the signal assignable to the thiocarbonyl C²=S carbon, at 181.0 ppm, whereas the respective signals in the spectrum of thiopyran **6** are present at 156.7 (C⁶), 159.3 (C⁴), and 160.4 (C²) ppm.

Scheme 3.
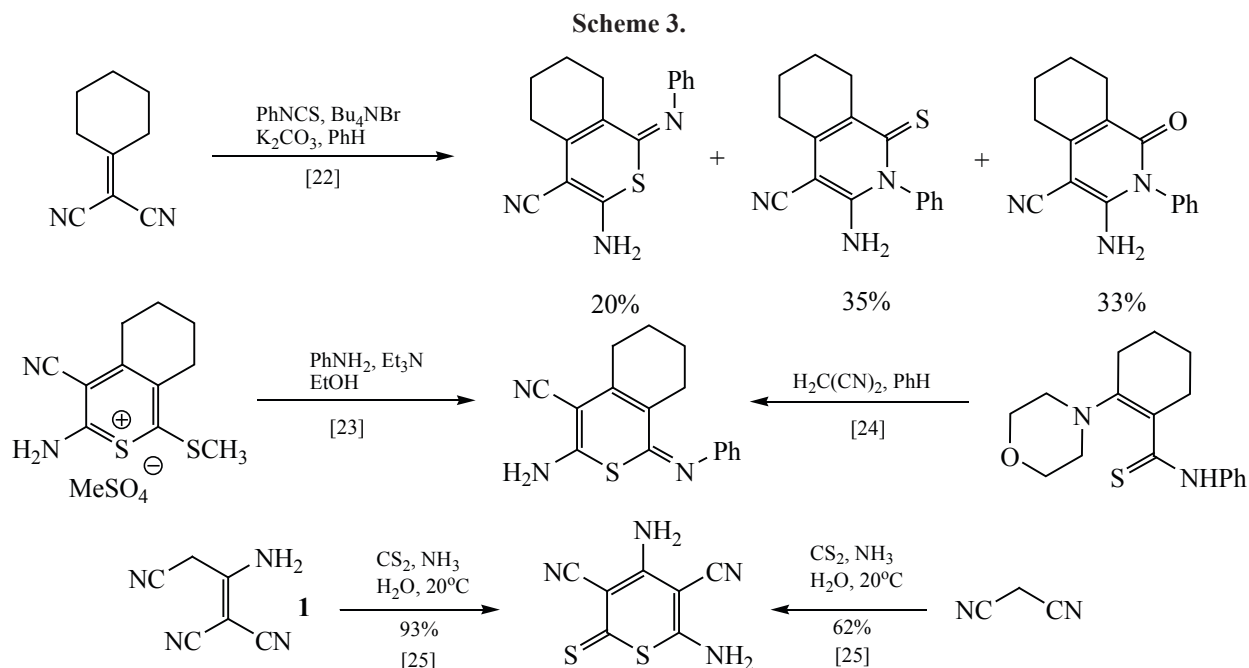
The IR spectra of compounds **2**, **5**, and **6** contain stretching vibration bands of the N–H bonds and conjugated C≡N groups (2204–2212 см$^{-1}$). At the same time, the spectra of thiones **2** and **5** show vibration bands of the C=S bond (strong bands at 1344–1348 cm^{-1} and medium intensity bands at 1180–1190 cm^{-1}).

Quantum-chemical study. Further evidence for the structure of compounds **2**, **5**, and **6** was obtained by the quantum-chemical calculations of spectral modes. For example, the molecular geometry (Fig. 1) and IR spectra, calculated using the ORCA 4.2 software package [26, 27], at the B3LYP–D3BJ level of theory [28–31] with the 6-311+G(2d,p) split-valence basis set, showed

a good fit to the experimental spectra (Tables 2 and 3). The calculated and experimental frequencies were compared using scale factors [0.9679 for high-frequency (>1000 cm^{-1}) and 1.0100 for low-frequency modes (<1000 cm^{-1})] [32]. The input files were generated using the Gabedit 2.5 program [33]. The ChemCraft 1.8 program was used to visualize the molecular geometries and calculated IR spectra.

Quantum-chemical calculations were also applied to interpret the experimental results, in particular, the different regioselectivities of the heterocyclizations of phenyl isothiocyanate with malononitrile dimer. The mechanisms of intramolecular cyclization were calculated

Table 2. Comparison of the principal absorption bands in the experimental and calculated IR spectra of 4,6-diamino-2-thioxo-1-phenyl-1,2-dihydropyridine-3,5-dicarbonitrile **2**

| Assignment	Experimental absorption bands, ν, cm^{-1}	Calculated absorption bands, ν, cm^{-1}	
		corrected	uncorrected
ν_{as}(N–H)	3336.4, 3301.7	3705.4, 3693.3	3586.5, 3574.7
ν_s(N–H)	3211.1	3583.0, 3569.6	3468.0, 3455.0
ν(C≡N)	2206.3	2297.7, 2283.3	2223.9, 2210.0
δ(NH$_2$)	1635.4	1659.1, 1646.0	1605.9, 1593.2
Skeletal ν(C=C)	1564.1, 1523.6, 1485.0	1585.1, 1532.5, 1527.1	1534.2, 1483.3, 1478.1
ν(C–N)	1454.1	1483.6	1436.0
ν(C=S)	1348.1	1366.7	1322.8
Skeletal	1222.7, 1180.3	1234.3, 1178.2	1194.7, 1140.4
ν(C=S)	1029.9	1052.2	1018.5
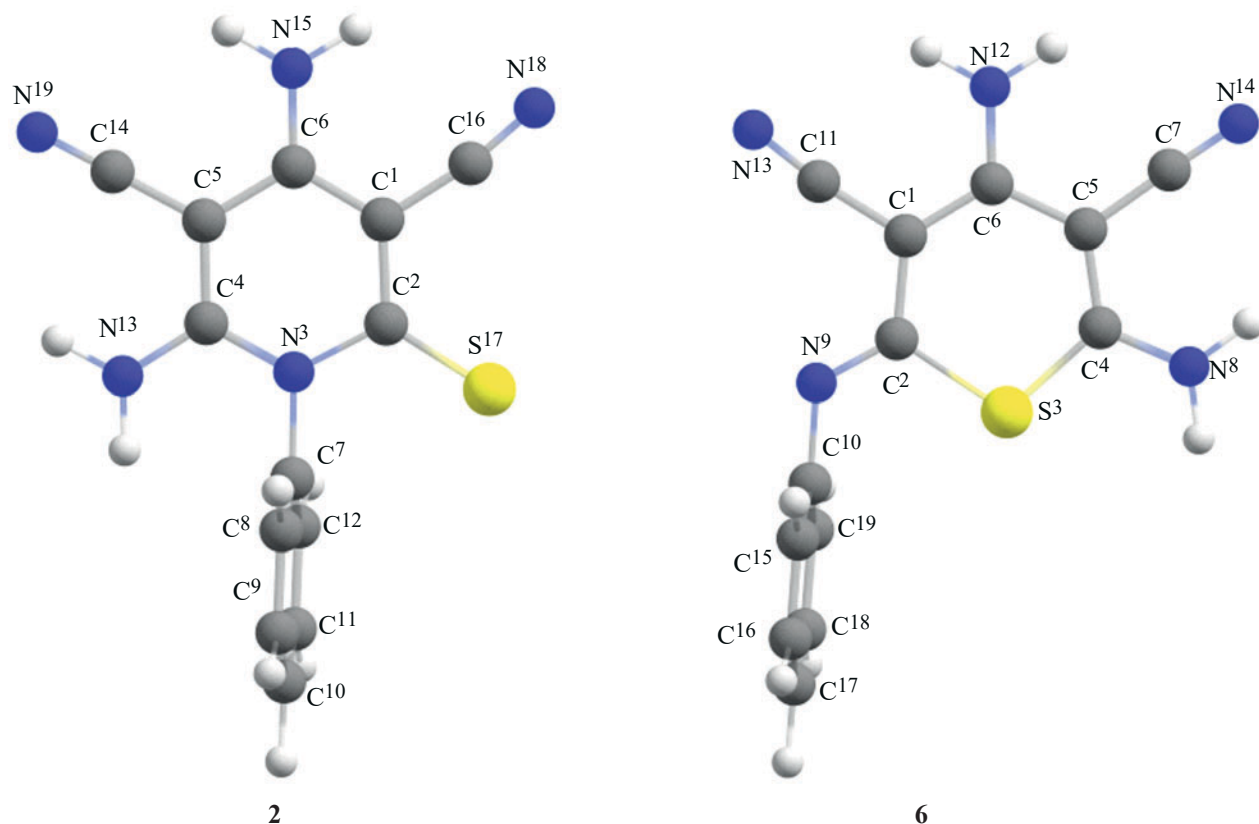
Fig. 1. Optimized structures of the cyclization products [calculation at the B3LYP-D3BJ/6-311+G(2d,p) level].

using the ORCA 4.2 software package [26, 27]. The search for transition states and reaction paths, as well as calculation of the vibration modes and Gibbs free energies were performed using the DFT method with the Grimme B97-3c scheme [34, 35], which combines the B97 GGA functional and the def2-mTZVP basis set with the D3BJ dispersion correction [36]. The obtained

transition state geometry was confirmed by the presence of an imaginary vibration frequency corresponding to the reaction coordinate. All calculations were performed with the inclusion of nonspecific solvation in the framework of the CPCM model [37].

To find out what of the two variants of the cyclization reaction (leading to 2-thioxopyridine **2** or to

Table 3. Comparison of the principal absorption bands in the experimental and calculated IR spectra of 4,6-diamino-2-(phenylimino)-2*H*-thiopyran-3,5-dicarbonitrile **6**

Assignment	Experimental absorption bands, ν, cm^{-1}	Calculated absorption bands, ν, cm^{-1}	
		corrected	uncorrected
ν_{as}(N–H)	3351.8, 3326.8	3700.4, 3694.6	3581.6, 3576.0
ν_{s}(N–H)	3234.2	3572.3 , 3570.8	3457.7, 3456.1
ν(C≡N)	2212.1	2291.9 , 2281.6	2218.4, 2208.4
ν(C=N)	1643.1	1681.4	1627.4
δ(NH$_2$)	1604.6	1662.0, 1652.9	1608.6, 1599.9
ν(C=C)	1564.7,	1629.3,	1577.0,
Skeletal	1521.6, 1488.9	1580.7, 1513.0	1529.9, 1464.5
ν(C–N)	1456.1	1448.4	1401.9
Skeletal	1282.5, 1153.3	1327.1, 1234.4	1284.5, 1194.8

Scheme 4.
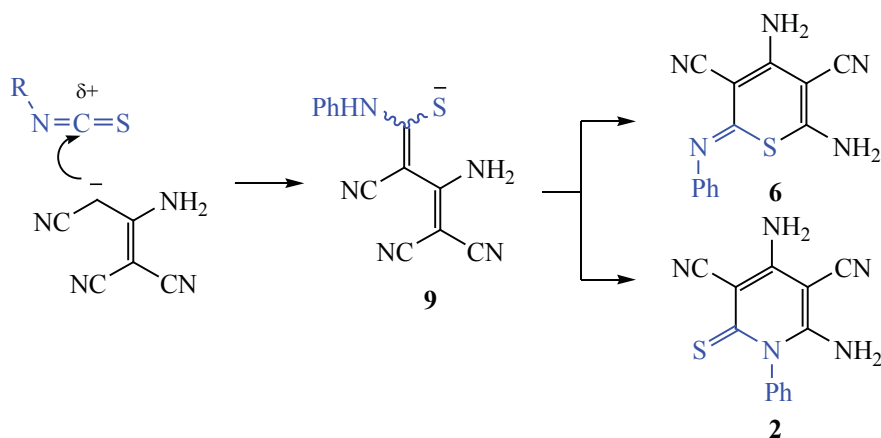
2-iminothiopyran **6**), we compared the calculated reaction paths. The obvious intermediate, both for pyridine **2** and for thiopyran **6**) is anion **9** formed by the nucleophilic attack of the anion of malononitrile dimer on the central carbon atom of isothiocyanate (Scheme 4).

Since the reaction was carried out with an excess of a base (triethylamine) in ethanol or pyridine (as a solvent), as the initial structure we considered anion **9** associated with two base molecules, one of which was protonated and thus formed an ion pair with anion **9** and the second was hydrogen-bonded to the H^{22} proton (Fig. 2a). To determine the optimal geometry of the initial state, a search was for the most stable conformation of anion **9** was first performed.

The cyclization leading to 2-thioxopyridine **2** occurs as a result of the nucleophilic attack of N^{13} on C^6, accompanied by H^{45} transfer from the base molecule to N^8 and deprotonation of N^{13} by the second base (triethylamine or pyridine) molecule (Figs. 2b and 2d). The reaction leading to thiopyran **6** involves the nucleophilic attack of S^{12} on C^6, accompanied by proton transfer from the base molecule to N^8 (Figs. 2c and 2e). The subsequent deprotonation of N^{13} by the second base molecule has, according to the calculations, very low activation energy, and, therefore, it is not a rate-limiting stage.

The molecular structures of starting anion **9**, transition states, and cyclization products are presented in Fig. 2 (reaction in pyridine). The calculations showed that the cyclization leading to thiopyran **6** is a kinetically controlled reaction. The activation energy is 70.2 kJ/mol. At the same time, the heat effect of this reaction is low (–9.1 kJ/mol). The activation energy of the cyclization,

leading to 2-thioxopyridine **2**, is 91.5 kJ/mol, but its heat effect is higher (–36.6 kJ/mol). Thus, under the thermodynamic control, 2-thioxopyridine **2** should be the main reaction product.

The simulation of analogous process in the ethanol medium (the resulting molecular structures are presented in Fig. 3) showed that the activation energy of the cyclization reaction in the presence of triethylamine as a base increases to 138.2 kJ/mol, and the heat effect of this reaction also increases (–48.2 kJ/mol). Presumably, the reason why this process has a higher activation energy compared to the same reaction in pyridine is the mutual repulsion of the two bulky triethylamine molecules, which are getting closer together during reaction, and the resulting distortion of the molecular structure of the reacting substrate. Thus, the benzene ring on the N^{13} atom takes a position almost perpendicular to the forming pyridine ring. The cyclization involving the sulfur atom, while having a slightly lower activation energy (65.2 kJ/mol), has a negative heat effect (4.5 kJ/mol), and, therefore, it is unlikely to occur. The energy profiles of the cyclization reactions in study are shown in Fig. 4.

Thus, having considered the simulated cyclization mechanisms allow us to conclude that 2-iminothiopyrans are formed under kinetic control, whereas 2-thioxo-pyridines are formed under thermodynamic control. The observed formation of 2-iminothiopyran in pyridine (25°C to refluxing) can be explained by the fact that initially, still at 25°C (before heating is applied), the reaction occurs under kinetically controlled conditions to form 2-iminothiopyran **6** which further is unable to undergo recyclization into 2-thioxopyridine **2** (the difficulty of the latter process was confirmed experimentally). The
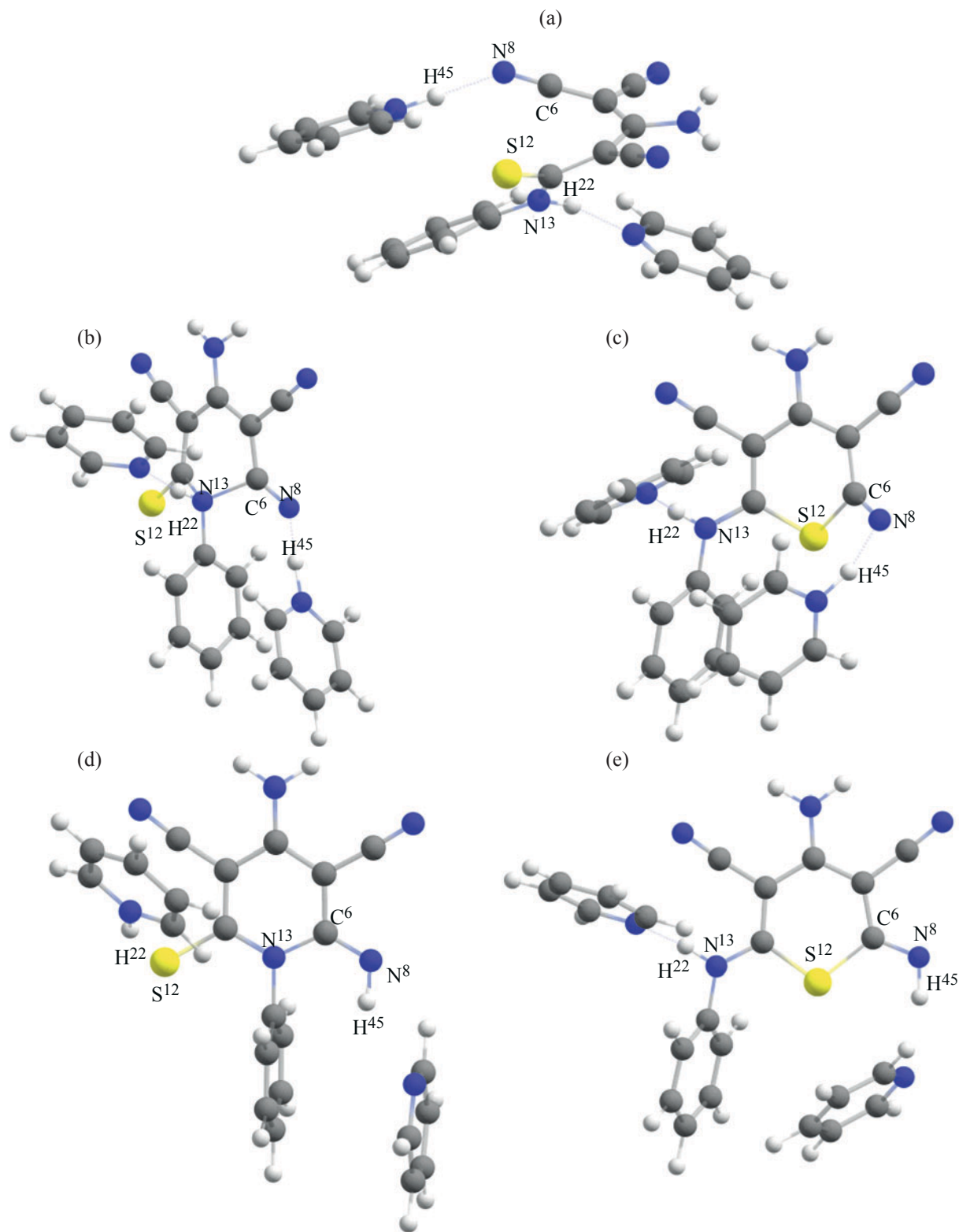
Fig. 2. Molecular structures of (a) starting anion **9** associated with two pyridine molecules, (b, c) transition states of the cyclization reactions and products of the cyclization by the (d) nitrogen atom N^{13} and (e) sulfur atom S^{12} (geometry optimization at the B97-3c level).
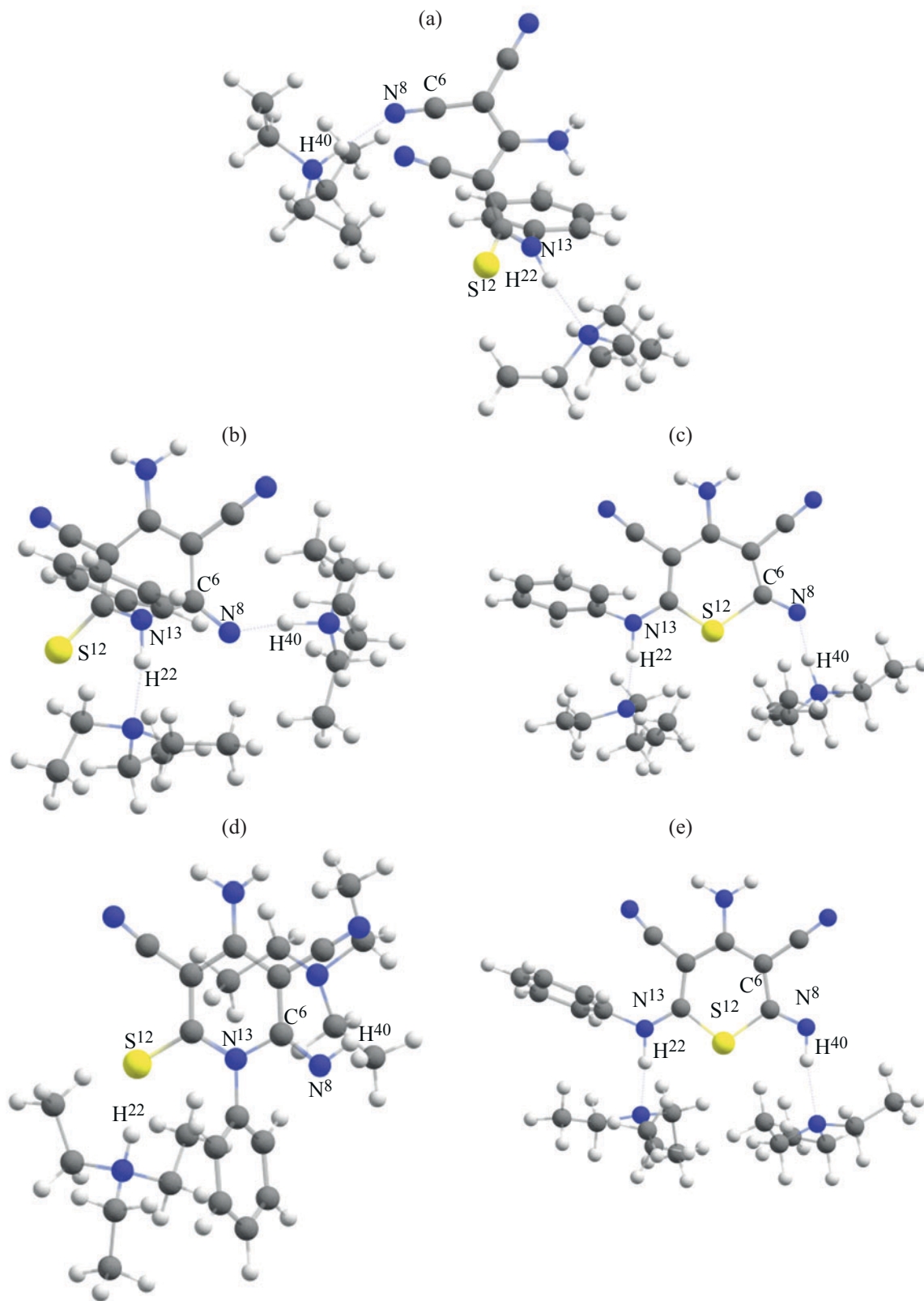
Fig. 3. Molecular structures of (a) starting anion **9** associated with two triethylamine molecules, (b, c) transition states of the cyclization reactions and products of the cyclization by the (d) nitrogen atom N^{13} and (e) sulfur atom S^{12} (geometry optimization at the B97-3c level).

different regioselectivities of the reactions of PhNCS with malononitrile dimer (Et$_3$N, EtOH, 25°C) and with its potassium salt (EtOH, 25°C) can be explained by a specific role of the base catalyst. Successful formation of 2-thioxopyridine **2** requires involvement of two base molecules: to form an unstable multi-charged transition state **10** (Scheme 5) requires simultaneous deprotonation of the endocyclic nitrogen atom with a free base and protonation of the negatively charged exocyclic nitrogen atom with the pyridinium (triethylammonium) cation.

However, in the case of malononitrile dimer salt **8**, such base and its protonated form are absent from the reaction medium. Water and ethanol, that are present in the reaction medium, are weaker proton donor/acceptors than pyridine or triethylamine and their conjugate acids; therefore, in this case, the reaction proceeds exclusively by the way of formation of kinetic product **6**.

In our opinion, the different results obtained with allyl isothiocyanate can be associated with more facile recyclization of the 2-iminothiopyran product. However, this issue calls for a more detailed study, which will be the subject of our further research.

***In silico* assessment of biological activity.** 6-Amino-2-thioxopyridine-3,5-dicarbonitriles and their derivatives exhibit broad-spectrum biological activity (see reviews [38–42] and recent works [43–48]), which makes them promising objects for study. The biological activity of 2-aminothiopyran-3,5-dicarbonitriles was also reported [49–51]. We performed a predictive analysis and *in silico* calculations of the potential targets, ADMET parameters, and compliance with the bioavailability parameters for compounds **2**, **5**, and **6**. Analysis of the structures of compounds **2**, **5**, and **6** for the compliance with Lipinski's rule of five [molecular weight (MW) ≤ 500, *c*Log*P* ≤ 5.0, TPSA ≤ 140 Å^2, H-bond acceptors ≤ 10, H-bond donors ≤ 5] [52–54] was performed using the OSIRIS Property Explorer software package [55]. The following parameters were calculated: *c*Log*P* [logarithm of the
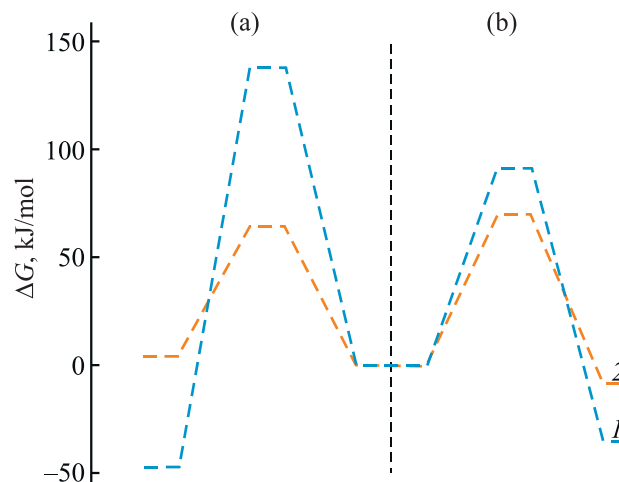

Fig. 4. Energy profiles of the cyclization reactions by the (*1*) nitrogen atom N^{13} and (*2*) sulfur atom S^{12} in (a) ethanol with triethylamine and (b) pyridine.

n-octanol/water partition coefficient log ($c_{\text{octanol}}/c_{\text{water}}$)], solubility (log *S*), topological polar surface area (TPSA), toxicity parameters: risks of side effects (mutagenic, oncogenic, and reproductive effects), parameter of similarity to known drugs (drug likeness), as well as general pharmacological assessment of a compound (drug score). The calculated data are presented in Table 4.

As we can see from the data in Table 4, the *c*Log*P* values for compounds **2**, **5**, and **6** vary from –0.95 to –0.13, which suggests good absorption and permeation [52–54]. At the same time, the log *S* value of lower than –4.0 for compound **2** points to a lower solubility (<1×10^{-4} M). The TPSA parameters for all the compounds have borderline values, even though they all formally fit the oral bioavailability criteria. No toxicity risks predicted for compounds **2**, **5**, and **6**. The drug likeness indices are low, but the drug scores, due to the formal compliance with the bioavailability criteria and predicted low toxicity, are fairly high (0.37–0.48).
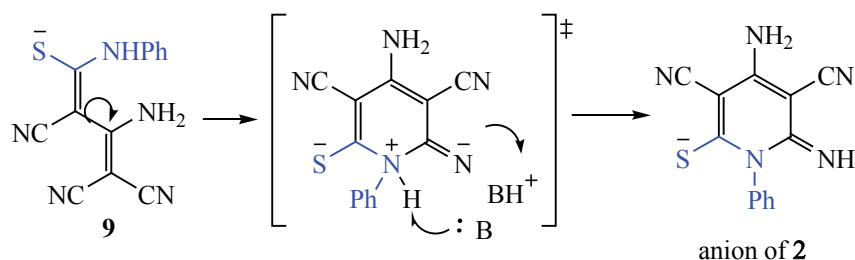
Scheme 5.

Table 4. Toxicity risks and physicochemical parameters of compounds **2**, **5**, and **6**, predicted by OSIRIS Property Explorer

Comp. no.	Toxicity risks[a]				Physicochemical parameters					
	A	B	C	D	cLog$P$	log$S$	MW	TPSA	drug likeness	drug score
2	−	−	−	−	−0.13	−5.14	267	134.9	−2.83	0.37
5	−	−	−	−	−0.95	−3.81	231	134.9	−4.92	0.44
6	−	−	−	−	−0.23	−2.79	267	137.2	−3.35	0.48

[a] (−) Predicted lack of toxicity: (A) mutagenicity, (B) carcinogenicity, (C) irritating effect, and (D) reproductive effects.

Table 5. Calculated ADMET parameters for compounds **2**, **5**, and **6**

Comp. no.	Penetration through BBB[a]	Gastrointestinal absorption[a]	Inhibition of cytochromes P450[a]					Acute toxicity (rats), LD50, $\log_{10}$ (mmol/kg)			
			CYP1A2	CYP2C19	CYP2C9	CYP2D6	CYP3A4	IP[b]	IV[b]	Oral[b]	SC[b]
2	−	+	+	−	+	−	+	−0.054	−0.403	0.316	0.006
								235.4	105.4	551.9	270.0
5	−	+	+	−	−	−	−	0.208	−0.178	0.601	0.083
								373.0	153.4	922.5	279.7
5	−	+	+	−	−	−	−	0.170	−0.250	0.375	0.413
								395.5	150.2	634.5	691.7

[a] (+) or (−) Presence or the lack.
[b] Administration route: (IP) intraperitoneal, (IV) intravenous, (Oral) peroral, and (SC) subcutaneous.
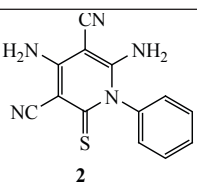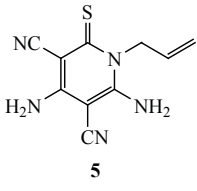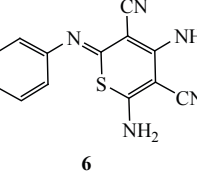
To predict biological activity, we also used the open source software PASS Online [56, 57] and AntiBac-Pred [58]. The resulting data predict an inhibitory effect on kinases for compound **2** with a probability of 0.765, an anti-ischemic effect for compound **5** with a probability of 0.800, as well as activity against the β-amyloid precursor protein for thiopyran **6** with a probability of 0.800. The highest antibacterial effect with respect to *Campylobacter jejuni* bacteria is predicted for compound **6** (confidence 0.3158; confidence > 0, if the probability of activity is greater than the probability of inactivity $P_a > P_i$).

The SwissADME [59, 60] and GUSAR [61, 62] software packages were used to predict the ADMET parameters (absorption, distribution, metabolism, excretion, toxicity). According to the US EPA criteria, in terms of acute oral toxicity, compounds **2**, **5**, and **6** can be assigned to class III (for low toxicity compounds, 500 mg/kg < LD$_{50}$ < 5000 mg/kg). Gastroenteric absorption, lack of ability to penetrate the blood–brain barrier (BBB), as well as lack of inhibition of most P450 cytochromes are predicted for all the compounds (Table 5).

The potential protein targets for the synthesized compounds were predicted using the new GalaxySagittarius protein–ligand docking protocol [63] based on the GalaxyWeb web server [64, 65]. The geometry and minimum energy optimized 3D structures of compounds **2**, **5**, and **6** were generated using the ORCA 4.2 software package [26, 27]. Docking using the GalaxySagittarius protocol was performed in the Binding compatability prediction and Re-ranking using docking modes. Table 6 shows the docking results compounds **2**, **5**, and **6** for 10 target–ligand complexes with the minimal free binding energies ΔG_{bind} and the best estimates for the protein–ligand interaction. The predicted protein targets are specified using the ID identifiers in the Protein Data Bank (PDB) and the UniProt database.

As we can see from Table 6, compounds **2**, **5**, and **6** show affinity to a wide range of proteins. In particular, the compounds are predicted to be the most affine urokinase plasminogen activator (uPA, PDB ID 1c5z, UniProt ID P00749) (Fig. 5), BRPF1 protein (PDB ID 5eww, UniProt ID P55201), and bromodomain-containing

Table 6. Predicted protein–ligand interactions for compounds **2**, **5**, and **6**

Compound	PDB ID protein identifier	UniProt ID protein identifier	Predock score	Docking score, kcal/mol	General protein–ligand binding predictor
2	**1c5z**	P00749	0.151	−13.995	0.256
	5eww	P55201	0.118	−15.877	0.237
	5ji8	Q9H8M2	0.113	−15.024	0.226
	6aaj	O60674	0.108	−15.379	0.223
	5up3	Q99683	0.101	−16.102	0.221
	4awo	P07900,P07900	0.093	−17.078	0.221
	6n0p	P15056,P15056	0.093	−16.679	0.218
	6i8z	Q05397	0.087	−17.038	0.214
	2hz0	P00519	0.090	−16.485	0.213
	4xs2	Q9NWZ3	0.093	−15.803	0.211
5	**1c5z**	P00749	0.225	−12.952	0.322
	5ji8	Q9H8M2	0.143	−13.354	0.244
	5eww	P55201	0.129	−13.502	0.230
	4ury	P01112,Q07889	0.114	−14.520	0.223
	3tiy	P24941	0.116	−13.489	0.217
	5v19	Q99683	0.107	−13.663	0.210
	5l3a	O60674	0.113	−12.772	0.209
	3ii5	P15056,P15056	0.108	−13.024	0.206
	4xs2	Q9NWZ3	0.110	−12.609	0.205
	2hz0	P00519	0.104	−13.084	0.202
6	**1c5z**	P00749	0.152	−14.802	0.263
	5ji8	Q9H8M2	0.117	−15.045	0.230
	5eww	P55201	0.120	−14.435	0.228
	5up3	Q99683	0.105	−15.935	0.224
	4hge	O60674	0.107	−14.178	0.214
	5hid	P15056,P15056	0.091	−16.337	0.213
	6i8z	Q05397	0.087	−16.488	0.210
	4xs2	Q9NWZ3	0.095	−15.140	0.208
	5ax9	Q9UKE5	0.074	−17.164	0.203
	4idv	Q99558	0.087	−15.332	0.202

protein 9 BRD9 (PDB ID 5ji8, UniProt ID Q9H8M2), which regulates the apoptosis signal to kinase 1 ASK1/MAP3K (PDB ID 5up3, UniProt ID Q99683) and a number of other targets. Considering the important role of uPA [66] and BRD9 [67] in oncogenic processes and of ASK1/MAP3K protein kinases in the immune response [68], the synthesized compounds can be considered as inhibitors potentially useful for treating various forms of cancer, neurodegenerative processes, rheumatoid arthritis, etc. In general, the results of the study allow us to conclude the following. The reaction of malononitrile dimer with isothiocyanates can take two different paths to form 4,6-diamino-2-thioxo-1,2-dihydropyridine-3,5-dicarbonitrile or 4,6-diamino-2-(phenylamino)-2*H*-thiopyran-3,5-dicarbonitrile. It should be noted that the formation of pyrimidine derivatives, reported in [9], has not been confirmed. Quantum-chemical calculations established that 2-iminothiopyrans and 2-thioxopyridines are formed under kinetically and thermodynamically controlled conditions, respectively. In the case of phenyl isothiocyanate, the reaction is regiocontrolled, and can be directed, by changing conditions, to the exclusive formation of a derivative of 2-(phenylimino)thiopyran or 2-thioxo-1-phenylpyridine. The predictive analysis of biological activity provide evidence showing that the synthesized compounds hold promise as potential pharmaceuticals.

EXPERIMENTAL

The IR spectra were obtained on a Bruker Vertex 70 spectrophotometer equipped with an ATR unit with a diamond crystal, accuracy ±4 cm^{-1}. The NMR spectra were recorded on a Bruker Avance III HD 400 MHz instrument (400.17 MHz for ^{1}H and 100.63 MHz for
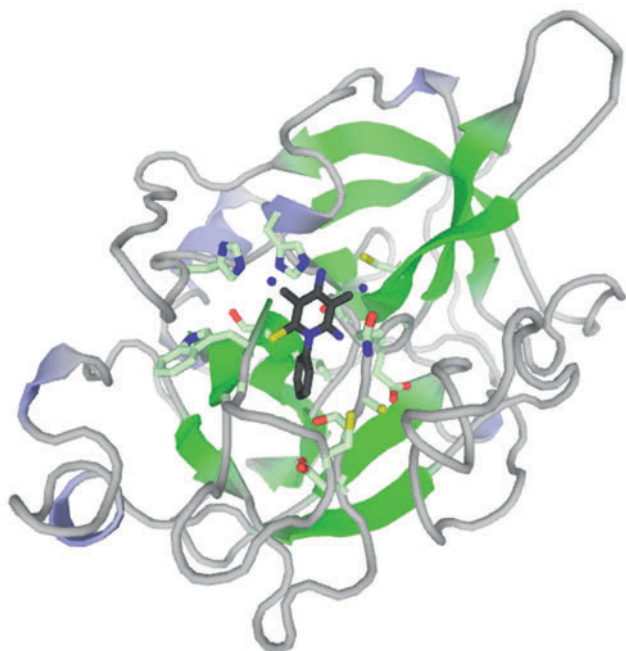
Fig. 5. Predicted structure of the protein–ligand complex of compound **2** and urokinase plasminogen activator (uPA, PDB ID 1c5z) (obtained with the GalaxySagittarius protocol).

^{13}C) in DMSO-d_6; the residual solvent signals were used reference. The purity of the synthesized compounds was controlled by TLC on Sorbfil-A plates (Imid, Krasnodar), eluent acetone–hexane (1: 1), visualization by exposure to iodine vapor and UV light.

Malononitrile dimer **1** was prepared according to Mittelbach [1]. Malononitrile dimer potassium salt **8** was prepared by the same procedure (yield 75–90%) but without final acidification, and the product was reacted without additional purification. Pyridine was dried over KOH.

4,6-Diamino-1-phenyl-2-thioxo-1,2-dihydro-pyridine-3,5-dicarbonitrile (2). *a. Synthesis from malo-nonitrile dimer 1 in the presence of Et$_3$N.* Triethylamine (1.05–1.6 mL, 7.57–11.35 mmol), was added to a stirred suspension of malononitrile dimer **1** (1.0 g, 7.57 mmol) in 15 mL of 96% ethanol. The mixture was stirred for 3–5 min until it homogenized completely or partially, after which PhNCS (0.91 mL, 7.57 mmol) was added. In about 5–10 min, a yellow precipitate started to form, and within 3–4 h the mixture thickened completely. It was allowed to stand for 24 h, after which the precipitate was filtered off, refluxed for 2 min in ethanol, filtered off, and washed with warm EtOH. Yield 1.70–1.86 g (84–92%), yellow powder, mp > 300°C {mp 250–252°C (AcOH) [5]}. IR spectrum, ν, cm^{-1}: 3456 w, 3414 w, 3367 m, 3336 m,

3302 s, 3211 s, br (N–H), 2206 s (C≡N), 1348 s, 1180 m (C=S). ^{1}H NMR spectrum, δ, ppm: 7.19–7.21 m (2H, H^2, H^6, Ph), 7.31 br. s (4H, NH$_2$), 7.43–7.53 m (3H, H^3–H^5, Ph). ^{13}C NMR spectrum (DEPTQ), δ$_C$, ppm: 67.3 (C^5), 88.1 (C^3), 114.5 (C≡N), 116.9 (C≡N), 129.1* (C^{2}H C^{6}H Ph), 129.5* (C^{4}H Ph), 130.1* (C^{3}H C^{5}H Ph), 137.7 (C^1 Ph), 155.6 (C^4 or C^6), 155.9 (C^6 or C^4), 181.0 (C=S). Here and hereinafter, the *asterisk* marks the out-of-phase signals. Found, %: C 58.44; H 3.46; N 26.13. C$_{13}$H$_9$N$_5$S. Calculated, %: 58.41; H 3.39; N 26.20. *M* 267.31.

b. Synthesis from malononitrile dimer 1 in boiling pyridine. Compound **2** was prepared by the procedure in [9], described as a method of synthesis of 6-amino-1-phenyl-2-thioxo-1,2,3,4-tetrahydropyrimidin-4-ylidene)-malononitrile. A mixture of PhNCS (1.2 mL, 0.01 mol) and malononitrile dimer **1** (1.32 g, 0.01 mol) in 30 mL of anhydrous pyridine was heated under reflux for 2 h and then cooled. The resulting dark blue solution was poured onto ice, acidified with HCl to pH 2, and was allowed to stand in a refrigerator at 4°C for 24 h. The yellow precipitate that formed was filtered off, washed with water and EtOH, and refluxed for 3–5 min in EtOH for purification. The yellow–orange precipitate was filtered off to obtain 2-thioxopyridine **2**. Yield 48%, mp > 300°C. The spectral characteristics are the same as above.

1-Allyl-4,6-diamino-2-thioxo-1,2-dihydropyridine-3,5-dicarbonitrile (5). *a. Synthesis from malononitrile dimer 1.* Triethylamine (1.05–1.6 mL, 7.57–11.35 mmol), was added to a stirred suspension of malononitrile dimer **1** (1.0 g, 7.57 mmol) in 15 mL of 96% ethanol. The mixture was stirred until homogeneous, after which allyl isothiocyanate (0.75 mL, 7.66 mmol) was added. The resulting mixture was stirred for 2 h and then left to stand for 24 h to let it to crystallize completely. The precipitate was filtered off and washed with EtOH. Yield 1.00–1.10 g (58–73%), colorless needle-like crystals, decomp. point 240°C. IR spectrum, ν, cm^{-1}: 3454 w, 3365 w, 3306 s, 3213 br. s (N–H), 2204 s (C≡N), 1344 s, 1190 m (C=S). ^{1}H NMR spectrum, δ, ppm: 4.95 d. d (1H, *trans*-CH$_2$, ^3J 17.4, ^2J 1.2 Hz), 5.09 d. d (1H, *cis*=CH$_2$, ^3J 10.5, ^2J 1.2 Hz), 5.28 br. s (2H, NCH$_2$), 5.71–5.81 m (CH$_2$CH=CH$_2$), 7.20 br. s (2H, C^{4}NH$_2$), 7.97 br. s (2H, C^{6}NH$_2$). ^{13}C NMR spectrum (DEPTQ), δ$_C$, ppm: 48.7 (NCH$_2$), 67.4 (C^5), 87.7 (C^3), 114.5 (C≡N), 115.7 (=CH$_2$), 117.1 (C≡N), 130.6* (CH$_2$CH=CH$_2$), 154.9 (C^4 or C^6), 155.2 (C^6 or C^4), 180.0 (C=S). Found, %: C 51.94; H 3.97; N 30.23. C$_{10}$H$_9$N$_5$S. Calculated, %: 51.93; H 3.92; N 30.28. *M* 231.28.

b. Synthesis from malononitrile dimer potassium salt **8**. Allyl isothiocyanate (0.5 mL, 5.09 mmol) and then 2 mL of water were added to a stirred suspension of 0.87 g (5.09 mmol) of salt **8** in 10 mL EtOH. A slight exotherm developed, and the mixture homogenized to form a tea-colored solution. A day after, a crystalline precipitate began to slowly form. In 3 days, the pale pink crystals were filtered off and washed with EtOH and petroleum ether. The product was spectrally identical to compound **5** prepared as described above. Yield 329 mg (28%). Attempted isolation of an additional amount of the product by addition water or acid to the mother liquor failed.

4,6-Diamino-2-(phenylimino)-2*H*-thiopyran-3,5-dicarbonitrile (6). *a. Synthesis from malononitrile dimer in pyridine.* A mixture of PhNCS (1.2 mL, 0.01 mol) and malononitrile dimer **1** (1.32 g, 0.01 mol) in 30 mL of anhydrous pyridine was allowed to stand for 24 h at 25°C and then refluxed for 2 h and cooled down. The resulting dark solution was poured onto ice, acidified to pH 2 with HCl, and allowed to stand in a refrigerator for 24 h at 4°C. The precipitate was filtered off, washed with EtOH, and refluxed for 3–5 min in EtOH for purification. The beige precipitate was filtered off to obtain 0.20 g (8%) of compound **6**, mp > 300°C {mp 225°C (EtOH) [9]}. IR spectrum, ν, cm^{-1}: 3427 w, 3410 w, 3371 m, 3352 m, 3329 m, 3234 s, ш (N–H), 2212 с (C≡N), 1643 m (C=N). ^{1}H NMR spectrum, δ, ppm: 7.11 br. s (2H, C^{4}NH$_2$), 7.18 br. s (2H, C^{6}NH$_2$), 7.24–7.27 m (2H, H^2, H^6, Ph), 7.48–7.54 m (3H, H^{3}H^5, Ph). ^{13}C NMR spectrum (DEPTQ), δ$_C$, ppm: 62.4 (C^5), 69.4 (C^3), 115.2 (C≡N), 116.6 (C≡N), 129.3* (C^{2}H, C^{6}H, Ph), 129.5* (C^{4}H, Ph), 130.0* (C^{3}H, C^{5}H, Ph), 134.1 (C^1, Ph), 156.7 (C^6), 159.3 (C^4), 160.4 (C^2). Found, %: C 58.40; H 3.50; N 26.15. C$_{13}$H$_9$N$_5$S. Calculated, %: 58.41; H 3.39; N 26.20. *M* 267.31.

b. Synthesis of malononitrile dimer potassium salt **8**. Phenyl isothiocyanate (3 mL, 0.0526 mol), was added to a stirred suspension of salt **8** (9.0 g, 0.0526 mol) in 135 mL of 96% ethanol.

Therewith, salt **8** quickly dissolved, and a yellow solution was formed. After ~2 h, a precipitate started to form. The mixture was stirred without heating for another 24 h. White powder of 2-iminothiopyran **6** was filtered off, washed with EtOH. Yield 11.57 g (82%). The product is spectrally identical to compound **6** obtained as described above.

AUTHOR INFORMATION

V.V. Dotsenko, ORCID: http://orcid.org/0000-0001-7163-0497

A.V. Bespalov, ORCID: http://orcid.org/0000-0002-9829-9674

A.A. Russkikh, ORCID: http://orcid.org/0000-0001-9354-9470

V.K. Kindop, ORCID: http://orcid.org/0000-0002-9005-9668

N.A. Aksenov, ORCID: http://orcid.org/0000-0002-7125-9066

I.V. Aksenova, ORCID: http://orcid.org/0000-0002-8083-1407

S.V. Shcherbakov, ORCID: http://orcid.org/0000-0003-3828-6641

S.N . Ovcharov, ORCID: http://orcid.org/0000-0002-4638-6098

CONFLICT OF INTEREST

No conflict of interest was declared by the authors.

OPEN ACCESS

SUPPLEMENTARY INFORMATION

The online version contains supplementary material available at https://doi.org/10.1134/S1070363221060013

REFERENCES

1. Mittelbach, M., *Monatsh. Chem.*, 1985, vol. 116, no. 5, p. 689.
https://doi.org/10.1007/BF00798796

2. Dotsenko, V.V., Krivokolysko, S.G., and Semenova, A.M., *Chem. Heterocycl. Compd.*, 2018, vol. 54, no. 11, p. 989.
https://doi.org/10.1007/s10593-018-2383-y

3. Shaabani, A. and Hooshmand, S.E., *Mol. Divers.*, 2018, vol. 22, no. 1, p. 207.
https://doi.org/10.1007/s11030-017-9807-y

4. Alekseeva, A.Yu. and Bardasov, I.N., *Chem. Heterocycl. Compd.*, 2018, vol. 54, no. 7, p. 689.
https://doi.org/10.1007/s10593-018-2332-9

5. Eldin, A.M.S., *Phosphorus, Sulfur, Silicon, Relat. Elem.*, 2003, vol. 178, no. 10, p. 2215.
https://doi.org/10.1080/713744561

6. El-Taweel, F.M., Elagamey, A.A., El-Kenawy, A.A., and Waly, M.A., *Phosphorus, Sulfur, Silicon, Relat. Elem.*, 2001, vol. 176, no. 1, p. 215.
https://doi.org/10.1080/10426500108055120

7. Mohareb, R.M., Sherif, S.M., and Samy, A.M., *Phosphorus, Sulfur, Silicon, Relat. Elem.*, 1995, vol. 101, nos. 1–4, p. 57.
https://doi.org/10.1080/10426509508042499

8. Mohareb, R.M., *Monatsh. Chem.*, 1992, vol. 123, no. 4, p. 341.
https://doi.org/10.1007/BF00810946

9. Abdel-Latif, E., Mustafa, H.M., Etman, H.A., and Fadda, A.A., *Russ. J. Org. Chem.*, 2007, vol. 43, no. 3, p. 443.
https://doi.org/10.1134/S1070428007030219

10. Dotsenko, V.V., Ismiev, A.I., Khrustaleva, A.N., Frolov, K.A., Krivokolysko, S.G., Chigorina, E.A., Snizhko, A.P., Gromenko, V.M., Bushmarinov, I.S., Askerov, R.K., Pekhtereva, T.M., Suykov, S.Yu., Papayanina, E.S., Mazepa, A.V., and Magerramov, A.M., *Chem. Heterocycl. Compd.*, 2016, vol. 52, no. 7, p. 473.
https://doi.org/10.1007/s10593-016-1918-3

11. Semenova, A.M., Oganesyan, R.V., Dotsenko, V.V., Chigorina, E.A., Aksenov, N.A., Aksenova, I.V., and Netreba, E.E., *Russ. J. Gen. Chem.*, 2019, vol. 89, no. 1, p. 19.
https://doi.org/10.1134/S1070363219010043

12. Dotsenko, V.V., Krivokolysko, S.G., and Semenova, A.M., *Chem. Heterocycl. Compd.*, 2018, vol. 54, no. 11, p. 989.
https://doi.org/10.1007/s10593-018-2383-y

13. Bakhite, E.A.-G., *Phosphorus, Sulfur, Silicon, Relat. Elem.*, 2003, vol. 178, p. 929.
https://doi.org/10.1080/10426500390208820

14. Paronikyan, Ye.G., Arutyunyan, A.S., and Dashyan, Sh.Sh., *Khim. Zh. Arm.*, 2017, vol. 70, nos. 1–2, p. 179.

15. Dotsenko, V.V., Buryi, D.S., Lukina, D.Yu., and Krivokolysko, S.G., *Russ. Chem. Bull.*, 2020, vol. 69, no. 10, p. 1829.
https://doi.org/10.1007/s11172-020-2969-2

16. Sajadikhah S.S. and Marandi, G., *Chem. Heterocycl. Compd.*, 2019, p. 1171.
https://doi.org/10.1007/s10593-019-02596-1

17. Akhmetova, V.R., Nadyrgulova, G.R., Niatshina, Z.T., and Dzhemilev, U.M., *Chem. Heterocycl. Compd.*, 2009, vol. 45, no. 10, p. 1155.
https://doi.org/10.1007/s10593-010-0403-7

18. Akhmetova, V.R. and Rakhimova, E.B., *Russ. J. Org. Chem.*, 2014, vol. 50, no. 12, p. 1711.
https://doi.org/10.1134/S107042801412001X

19. Dotsenko, V.V., Frolov, K.A., and Krivokolysko, S.G., *Chem. Heterocycl. Compd.*, 2015, vol. 51, no. 2, p. 109.
https://doi.org/10.1007/s10593-015-1668-7

20. Dotsenko, V.V., Frolov, K.A., Chigorina, E.A., Khrustaleva, A.N., Bibik, E.Yu., and Krivokolysko, S.G., *Russ. Chem. Bull.*, 2019, vol. 68, no. 4, p. 691.
https://doi.org/10.1007/s11172-019-2476-5

21. Dotsenko, V.V., Krivokolysko, S.G., and Chigorina, E.A., *Russ. J. Gen. Chem.* 2020, vol. 90, no. 4, p. 590.
https://doi.org/10.1134/S1070363220040052

22. El-Sayed, A.M. and Abdel-Ghany, H., *J. Heterocycl. Chem.*, 2000, vol. 37, no. 5, p. 1233.
https://doi.org/10.1002/jhet.5570370534

23. Gewald, K., Buchwalder, M., and Peukert, M., *J. Prakt. Chem.*, 1973, vol. 315, no. 4, p. 679.
https://doi.org/10.1002/prac.19733150413

24. Bogdanowicz-Szwed, K., *Monatsh. Chem.*, 1982, vol. 113, no. 5, p. 583.
https://doi.org/10.1007/BF00800265

25. Takeshima, T., Yokoyama, M., Fukada, N., and Akano, M., *J. Org. Chem.*, 1970, vol. 35, no. 7, p. 2438.
https://doi.org/10.1021/jo00832a085

26. Neese, F., *WIREs Comput. Mol. Sci.*, 2011, vol. 2, p. 73.
https://doi.org/10.1002/wcms.81

27. Neese F., *WIREs Comput. Mol. Sci.*, 2017, vol. 8, p. e1327.
https://doi.org/10.1002/wcms.1327

28. Becke, A.D., *Phys. Rev. A*, 1988, vol. 38, p. 3098.
https://doi.org/10.1103/PhysRevA.38.3098

29. Lee, C., Yang, W., and Parr, R.G., *Phys. Rev. B*, 1988, vol. 37, p. 785.
https://doi.org/10.1103/PhysRevB.37.785

30. Grimme, S., Antony, J., Ehrlich, S., and Krieg, H., *J. Chem. Phys.*, 2010, vol. 132, p. 154104.
https://doi.org/10.1063/1.3382344

31. Goerigk, L. and Grimme, S., *Phys. Chem. Chem. Phys.*, 2011, vol. 13, p. 6670.
https://doi.org/10.1039/C0CP02984J

32. Andersson, M.P. and Uvdal, P., *J. Phys. Chem. A*, 2005, vol. 109, p. 2937.
https://doi.org/10.1021/jp045733a

33. Allouche, A.-R., *J. Comput. Chem.*, 2011, vol. 32, p. 174.
https://doi.org/10.1002/jcc.21600.

34. Brandenburg, J.G., Bannwarth, C., Hansen, A., and Grimme, S., *J. Chem. Phys.*, 2018, vol. 148, p. 064104.
https://doi.org/10.1063/1.5012601

35. Caldeweyher, E. and Brandenburg, J.G., *J. Phys. Condens. Matter*, 2018, vol. 30, p. 213001.
https://doi.org/10.1088/1361-648X/aabcfb

36. Grimme, S., Ehrlich, S., and Goerigk, L., *J. Comput. Chem.*, 2011, vol. 32, p. 1456.
https://doi.org/10.1002/jcc.21759

37. Tomasi, J., Mennucci, B., and Cammi, R., *Chem. Rev.*, 2005, vol. 105, p. 2999.
https://doi.org/10.1021/cr9904009

38. Litvinov, V.P., Rodinovskaya, L.A., Sharanin, Yu.A., Shestopalov, A.M., and Senning, A., *J. Sulfur Chem.*, 1992, vol. 13, no. 1, p. 1.
https://doi.org/10.1080/01961779208048951

39. Litvinov, V.P., *Phosphorus, Sulfur, Silicon, Relat. Elem.*, 1993, vol. 74, no. 1, p. 139.
https://doi.org/10.1080/10426509308038105

40. Litvinov, V.P., *Russ. Chem. Bull.*, 1998, vol. 47, no. 11, p 2053.
https://doi.org/10.1007/BF02494257

41. Litvinov, V.P., Krivokolysko, S.G., and Dyachenko, V.D., *Chem. Heterocycl. Compd.*, 1999, vol. 35, no. 5, p. 509.
https://doi.org/10.1007/BF02324634

42. Litvinov, V.P., *Russ. Chem. Rev.*, 2006, vol. 75, no. 7, p. 577.
https://doi.org/10.1070/RC2006v075n07ABEH003619

43. Attia, A.M., Khodair, A.I., Gendy, E.A., El-Magd, M.A., and Elshaier, Y.A.M.M., *Lett. Drug Design Discov.*, 2020, vol. 17, no. 2, p. 124.
https://doi.org/10.2174/1570180816666190220123547

44. Catarzi, D., Varano, F., Varani, K., Vincenzi, F., Pasquini, S., Dal Ben, D., Volpini, R., and Colotta, V., *Pharmaceuticals*, 2019, vol. 12, no. 4, p. 159.
https://doi.org/10.3390/ph12040159

45. Schweda, S.I., Alder, A., Gilberger, T., and Kunick, C., *Molecules*, 2020, vol. 25, no. 14, p. 3187.
https://doi.org/10.3390/molecules25143187

46. Grigor'ev, A.A., Shtyrlin, N.V., Gabbasova, R.R., Zeldi, M.I., Grishaev, D. Yu., Gnezdilov, O.I., Balakin, K.V., Nasakin, O.E., and Shtyrlin, Y.G., *Synth. Commun.*, 2018, vol. 48, no. 17, p. 2288.
https://doi.org/10.1080/00397911.2018.1501487

47. Betti, M., Catarzi, D., Varano, F., Falsini, M., Varani, K., Vincenzi, F., Dal Ben, D., Lambertucci, C., and Colotta, V., *Eur. J. Med. Chem.*, 2018, vol. 150, p. 127.
https://doi.org/10.1016/j.ejmech.2018.02.081

48. Fugel, W., Oberholzer, A.E., Gschloessl, B., Dzikowski, R., Pressburger, N., Preu, L., Pearl, L.H., Baratte, B., Ratin, M., Okun, I., Doerig, C., Kruggel, S., Lemcke, T., Meijer, L., and Kunick, C., *J. Med. Chem.*, 2013, vol. 56, no. 1, p. 264.
https://doi.org/10.1021/jm301575n

49. Sanchez, M.I., de Vries, L.E., Lehmann, C., Lee, J.T., Ang, K.K., Wilson, C., Chen, S., Arkin, M.R., Bogyo, M., Deu, E., *PloS One*, 2019, vol. 14, no. 12, article no. e0226270.
https://doi.org/10.1371/journal.pone.0226270

50. Zhou, P. and Warren, J.D., WO Patent 2014031759, 2014.

51. Whitten, J.P., Pei, Y., Stauderman, K.A., and Roos, J., US Patent 2010087415, 2010.

52. Lipinski, C.A., Lombardo, F., Dominy, B.W., and Feeney, P.J., *Adv. Drug. Delivery Rev.*, 1997, vol. 23, nos. 1–3, p. 4.
https://doi.org/10.1016/S0169-409X(96)00423-1

53. Lipinski, C.A., *Drug Discov. Today: Technol.*, 2004, vol. 1, no. 4, p. 337.
https://doi.org/10.1016/j.ddtec.2004.11.007

54. Lipinski, C.A., Lombardo, F., Dominy, B.W., and Feeney, P.J., *Adv. Drug. Delivery Rev.*, 2012, vol. 64, Suppl. p. 4.
https://doi.org/10.1016/j.addr.2012.09.019.

55. Sander, T., *OSIRIS Property Explorer, Idorsia Pharmaceuticals*, Switzerland.
http://www.organic-chemistry.org/prog/peo/.

56. PASS Online. Laboratory for Structure-Function Based Drug Design, Institute of Biomedical Chemistry (IBMC), Moscow, Russia.
http://www.pharmaexpert.ru/passonline/predict.php.

57. Filimonov, D.A., Lagunin, A.A., Gloriozova, T.A., Rudik, A.V., Druzhilovskii, D.S., Pogodin, P.V., and Poroikov, V.V., *Chem. Heterocycl. Compd.*, 2014, vol. 50, no. 3, p. 444.
https://doi.org/10.1007/s10593-014-1496-1

58. Way2Drug. antiBac-Pred. Laboratory for Structure-Function Based Drug Design, Institute of Biomedical Chemistry (IBMC), Moscow, Russia.
http://way2drug.com/antibac/.

59. Daina, A., Michielin, O., and Zoete, V., *Sci. Rep.*, 2017, vol. 7, article no. 42717.
https://doi.org/10.1038/srep42717

60. Gfeller, D., Grosdidier, A., Wirth, M., Daina, A., Michielin, O., and Zoete, V., *Nucl. Acids Res.*, 2014, vol. 42, no. W1, p. W32.
https://doi.org/10.1093/nar/gku293

61. Lagunin, A., Zakharov, A., Filimonov, D., and Poroikov, V., *Mol. Informatics*, 2011, vol. 30, nos. 2–3, p. 241.
https://doi.org/10.1002/minf.201000151

62. GUSAR Online. Laboratory for Structure-Function Based Drug Design, Institute of Biomedical Chemistry (IBMC), Moscow, Russia.
http://www.way2drug.com/gusar/references.html.

63. Yang, J., Kwon, S., Bae, S.H., Park, K.M., Yoon, C., Lee, J.H., and Seok, C., *J. Chem. Inf. Model.*, 2020, vol. 60, no. 6, p. 3246.
https://doi.org/10.1021/acs.jcim.0c00104

64. GalaxyWEB. A web server for protein structure prediction, refinement, and related methods. Computational Biology Lab, Department of Chemistry, Seoul National University, S. Korea.
http://galaxy.seoklab.org/index.html

65. Ko, J., Park, H., Heo, L., and Seok, C., *Nucleic Acids Res.,* 2012, vol. 40, no. W1, p. W294.
https://doi.org/10.1093/nar/gks493

66. Katz, B.A., Mackman, R., Luong, C., Radika, K., Martelli, A., Sprengeler, P.A., Wang, J., Chan, H., and Wong, L., *Chem. Biol.*, 2000, vol. 7, no. 4, p. 299.
https://doi.org/10.1016/s1074-5521(00)00104-6

67. Clark, P.G., Vieira, L.C., Tallant, C., Fedorov, O., Singleton, D.C., Rogers, C.M., Monteiro, O.P., Bennett, J.M., Baronio, R., Müller, S., Daniels, D.L., Méndez, J., Knapp, S., Brennan, P.E., and Dixon, D.J., *Angew. Chem. Int. Ed.*, 2015, vol. 54, no. 21, p. 6217.
https://doi.org/10.1002/anie.201501394

68. Hayakawa, T., Matsuzawa, A., Noguchi, T., Takeda, K., and Ichijo, H., *Microb. Infect.*, 2006, vol. 8, no. 4, p. 1098.
https://doi.org/10.1016/j.micinf.2005.12.001